Check for updates

Evaluation of Patient-Specific Cranial Implant Design Using Finite Element Analysis

Stijn E.F. Huys[1], Anke Van Gysel[1], Maurice Y. Mommaerts[2], Jos Vander Sloten[1]

BACKGROUND: **Various studies have investigated the load-bearing capacity of patient-specific cranial implants. However, little attention has been given to the evaluation of the design of ceramic-titanium (CeTi) implants.**

METHODS: **A biomechanical evaluation of 3 patient-specific cranial implants was performed using finite element analysis.**

RESULTS: **The results of the analyses allowed the identification of the implant regions as well as the magnitudes of the maximum stresses on, and displacements along, these regions after traumatic impact. The analyses also showed that polyether ether ketone cranial implants offer inferior brain and neurocranial protection due to their high flexibility and local peak stresses at the bone-screw interface. In contrast, CeTi implants were able to evenly distribute the stresses along the interface and thus reduced the risk of neurocranial fracture. The scaffold structure at the border of these implants reduced stress shielding and enhanced bone ingrowth. Moreover, brain injuries were less likely to occur, as the CeTi implant exhibits limited deflection.**

CONCLUSIONS: **From the finite element analyses, CeTi cranial implants appear less likely to induce calvarial fractures with a better potential to protect the brain under impact loads.**

INTRODUCTION

Cranioplasty is a surgical reconstruction method that restores defects of the neurocranium using autogenous grafts or alloplastic materials.[1,2] The main goal of cranioplasty is to restore the protective function of the neurocranium, with a secondary goal of restoring craniofacial aesthetics and preventing the syndrome of the trephined.[1,3]

With recent advances in computer-aided design and computer-aided manufacturing techniques, the production of patient-specific cranial implants has increased. Patient-specific implants allow for a precise definition of the implant contour and curvature for each individual patient.[4] The material and type of fixation device are usually chosen according to the surgeon's preference, which is related to experience, availability, and cost. The materials can be categorized into autografts and bone substitutes, such as metals, polymers, and ceramics.[5,6] Numerous means of fixation exist as well, such as osteosynthetic plates or lips and tangential screws.[4,7] The optimized design of cranial implants is also of interest to increase surgical success, reduce the risk of complications, and obtain better aesthetic outcomes.

Numerical simulations, such as finite element analysis (FEA), have become important tools in biomedical engineering and for testing the safety of cranioplasty.[8,9] FEA allows the assessments of mechanical strength and shock resistance, and the identification of critical regions in the cranial implants or grafts without the need for mechanical testing. The outcome of the analysis can thus be used for implant design purposes.

The focus of this article is the evaluation of the design of 3 patient-specific cranial implants that were subjected to an impact

Key words
- Bone-implant interface
- Cranium
- Calcium phosphate
- Finite element analysis
- Patient-specific implant
- Polyether ether ketone
- Titanium

Abbreviations and Acronyms
BII: Bone-implant interface
BSI: Bone-screw interface
CeTi: Ceramic-titanium
FEA: Finite element analysis
ICP: Intracranial pressure
PEEK: Polyether ether ketone

From the [1]Engineering Science, Department of Mechanical Engineering, Section of Biomechanics, Catholic University of Leuven, Leuven; and [2]3D Innovations Laboratory, Universitair Ziekenhuis Brussel, Vrije Universiteit Brussel, Brussels, Belgium

To whom correspondence should be addressed: Maurice Y. Mommaerts, M.D., Ph.D. [E-mail: mauricemommaerts@me.com]

Citation: World Neurosurg. (2021) 148:■-■.
https://doi.org/10.1016/j.wneu.2021.01.102

*Journal homepage: **www.journals.elsevier.com/world-neurosurgery***

*Available online: **www.sciencedirect.com***

1878-8750/$ - see front matter © 2021 Elsevier Inc. All rights reserved.

load equivalent to a fall off a bicycle. The analyses focus on the maximum stresses on, and displacements along, the critical regions, which were identified as the bone-implant interface (BII) and the cranial area subjected to the impact.

MATERIALS AND METHODS

Three-dimensional models of the patient-specific cranial inlay implants and neurocraniums were provided by CADskills BV, Ghent, Belgium. The volume mesh was generated in 3-matic 13.0, which is part of the Mimics Innovation Suite (Materialise NV, Leuven, Belgium). The FEA was performed using Abaqus/CAE 6.14–1 (Dassault Systèmes, Paris, France).

Three global models were investigated: a polyether ether ketone (PEEK) cranial implant fixed with tangential screws and 2 ceramic-titanium (CeTi) cranial implants[10] fixed with tangential or axial screws, referred to as CeTi-TS and CeTi-AS, respectively. The CeTi cranial implants were constructed of a solid Ti_6Al_4V alloy (TiGr23 ELI) with a scaffolded border constructed of the same alloy into which HydroSet (Stryker CMF, Kalamazoo, Michigan, USA) was injected and sculpted. HydroSet is a fast-setting calcium phosphate paste that hardens to hydroxyapatite. Only part of the calvaria around the bone defect was used in the models to reduce the computational time of the simulations. Moreover, for each cranial implant, a local model was constructed as well. For this construction, a section of the global model was removed, with the screw fixation located centrally. This local model was subjected to a more comprehensive stress analysis.

Meshing Procedure

The meshing procedure is an important part of the FEA, as it allows the determination of the accuracy of the analytical results. A trade-off between accuracy and computational time was made for predictability and feasibility reasons. A coarse mesh decreases the accuracy, whereas a fine mesh increases the computational time.[3] A sensitivity analysis was also performed to determine the optimal mesh size, which was determined when the average von Mises stress was unable to alter the mesh more than 1% between simulations using different mesh densities.[8]

Table 1 provides the remeshing parameters for the 3 global models. Mesh refinement was performed at the BII and bone-screw interface (BSI), as a higher accuracy is desired at these critical regions. The meshing parameters for the local models were similar. The edge length of the scaffold was decreased to 0.4 mm, as the lattice structure of the scaffold was designed using local models. **Figure 1** shows the final mesh of the global and local CeTi-TS models, respectively. Similar meshes were obtained for the PEEK and CeTi-AS models.

Material Properties

All material properties were assumed to be linear elastic and isotropic. **Table 2** provides Young's modulus, Poisson's ratio, and strength of the different materials.

The material properties of the calvaria were calculated based on the average properties of the cortical and trabecular bones. The chosen Young's moduli of the cortical and trabecular bones were 15 GPa and 0.50 GPa, respectively, resulting in an average Young's modulus of 7.75 GPa. The average Poisson's ratio was equal to 0.30.[9]

The scaffold structure of the CeTi cranial implants consisted of 10% air, 10% Ti_6Al_4V, and 80% HydroSet. Based on these percentages, weighted averages of 11.50 GPa and 0.27 were used for Young's modulus and Poisson's ratio, respectively.

Table 1. Remeshing Parameters

	Edge Length (mm)	Influence Area (mm)	Growth Rate (%)
Cranial implant	1.5	0	25
Neurocranium	4.2	0	25
BII and BSI	1.2	5	25

BII, bone-implant interface; BSI, bone-screw interface.

Interaction Properties

The interaction properties between the implant and neurocranium were designed to maintain the highest physiological fidelity possible. It was assumed that the PEEK cranial implant and neurocranium would only make contact at the screw holes (BSI). Complete fixation was assumed due to the presence of tangential screws, which were modeled in Abaqus/CAE using the *hard contact* interaction property and the *tie constraint*. In the CeTi model, several interfaces required the assignment of interaction properties. The first interface was the BSI between the screw holes and the calvaria. The second interface was located between the solid Ti_6Al_4V region of the cranial implant and the calvaria (BII-solid). The third interface was located at the Ti scaffold containing the injected and sculpted HydroSet between the implant and

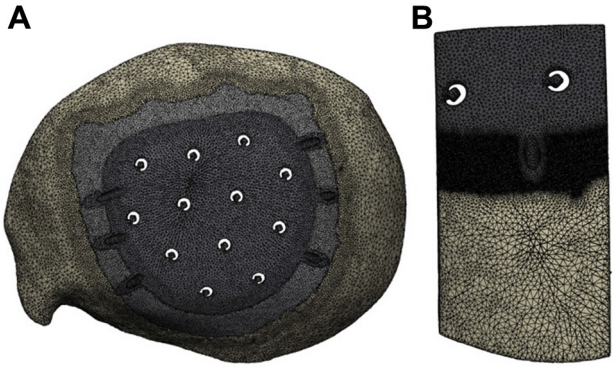

Figure 1. Mesh for the CeTi-TS global (**A**) and local (**B**) implant models. CeTi-TS, ceramic-titanium cranial implant fixed with tangential screw.

Table 2. Material Properties

Material	Young's Modulus (GPa)	Poisson's Ratio	Strength (MPa)	Reference
PEEK	4	0.36	115	Bogu et al[12]
Ti_6Al_4V	113	0.3	1301	Bogu et al[13]
HydroSet	0.25	0.3	24	Bogu et al[13] and Boyd et al[15]
Scaffold	11.5	0.27	149.3	Clarkin et al[14] and Boyd et al[15]
Bone	7.75	0.3	205	Safi et al[3] and Tsouknidas et al[9]

PEEK, polyether ether ketone.

neurocranium (BII-scaffold). Because of the osteoconductive behavior of the materials and the presence of screws, the *tie constraint* was used to model complete bonding along all of the interfaces.

Loading Conditions

Two static loads were applied to the global models; the first was an impact load representative of a fall off a bicycle. The load was modeled as a pressure acting perpendicular to a circular area with a radius of approximately 20 mm^2 (application area) centrally located on the implant. Based on a study by Fahlstedt et al,[11] the load should have a magnitude of 18 kN. The secondary load was a pressure of 25 mm Hg evenly distributed over the inner surface of the implant, which represents elevated intracranial pressure (ICP).

Boundary Conditions

The caudal side of the neurocranium in all 3 models was assumed to be completely anchored.[3] In Abaqus/CAE, the anchoring was modeled using the boundary condition *ENCASTRE*, which inhibits translation and rotation in all directions. The boundary conditions of the local models were based on the displacements along the corresponding nodes in the global models, as provided by the FEA. In this way, the loading conditions of the global models were imposed on the local models.

RESULTS

The results of the global models were used to analyze the maximum von Mises stress and displacement. The local models were used to analyze the maximum principal stress at the interface. Stress concentrations due to inaccuracies in the mesh density were ignored during the analyses. **Figure 2** shows the FEA outcomes for the impact load.

Global Models

Impact Load. The impact load led to the structural failure of the PEEK cranial implant and neurocranium. High local stress concentrations were seen at the BSI. These stresses were 1877.85 MPa and 1294.83 MPa on the cranial implant and neurocranium,

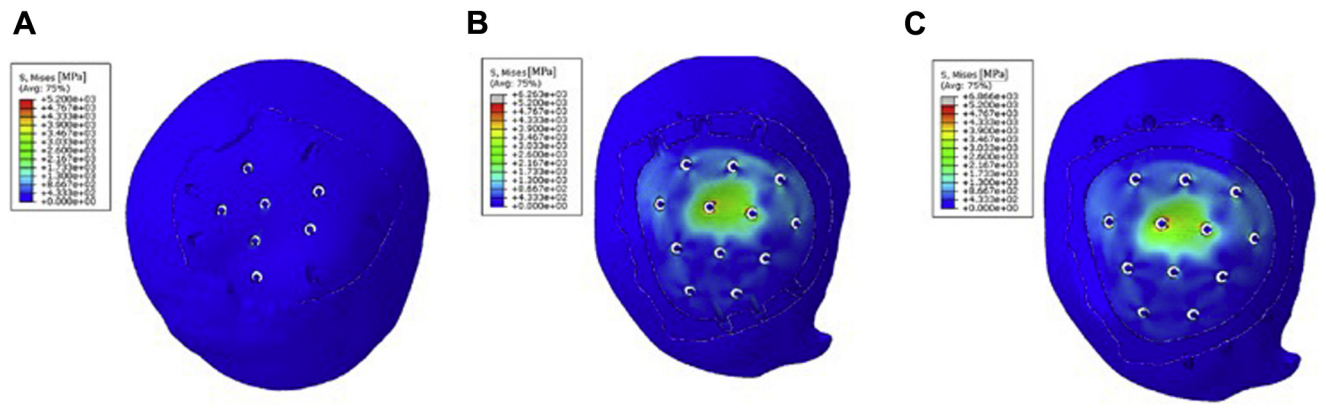

Figure 2. Displacement of von Mises stress along the 3 implant models related to impact load: (**A**) polyether ether ketone model, (**B**) CeTi-TS model, and (**C**) CeTi-AS model. CeTi-AS, ceramic-titanium cranial implant fixed with axial screw; CeTi-TS, ceramic-titanium cranial implant fixed with tangential screw.

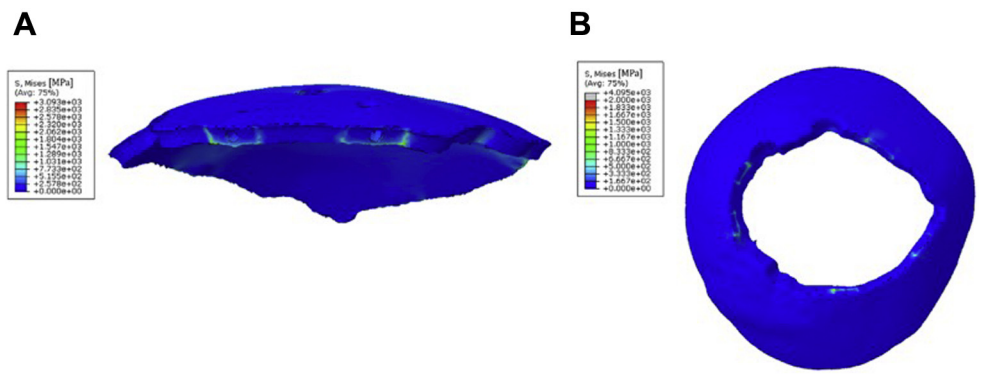

Figure 3. Results at the interface of the polyether ether ketone implant (**A**) and neurocranium (**B**) related to impact load.

respectively. The maximum stress values at the BII for both the implant and neurocranium were much smaller, as no fixation was present at this interface. The stress displacement along both the cranial implant and neurocranium is visualized in Figure 3.

The maximum stress on both CeTi implants was located at the application area. For both implants, the maximum stress was approximately 5100 MPa. As this stress value exceeds the strength of the Ti_6Al_4V alloy, structural failure at the center of the implant occurred, whereas the maximum stress on both the CeTi-TS and CeTi-AS neurocraniums did not exceed the bone strength. The stresses at the BSI, BII-solid, and BII-scaffold were much lower than those measured in the PEEK model and are visualized in Figure 4. The CeTi-TS model shows slightly higher stresses at the BSI in both the implant and neurocranium compared with the CeTi-AS model, whereas the stresses located at the BII-scaffold were equal in both CeTi models and were much smaller than the stress at the BII-solid.

The predominant deformation of the PEEK implant was bending at the contact zone where the impact occurred. The maximum deformation observed at the impact area of the PEEK implant was equal to 6.78 mm, whereas the maximum stress displacement along the CeTi models was also located at the application area and measured approximately 3.5 mm.

ICP. Similar local stress concentrations were measured in the PEEK model. Stresses were distributed along the CeTi implant interface when ICP was applied. The magnitudes of the stress and its displacement were not critical and did not lead to implant failure.

Local Models

Impact Load. The BSI of the PEEK cranial implant and neurocranium was subjected to maximum principal stress compression that exceeded the strength of the materials.

The BSI, BII-solid, and BII-scaffold of the CeTi-TS and CeTi-AS implants were subjected to tensile stresses that did not exceed the strength of the materials. The BII-solid of the neurocranium of the CeTi models was exposed to compression stresses that did not exceed the strength of the cranial bone. The maximum principal stress on the neurocranium at the BSI was tensile stress for both CeTi models, which, in the case of the CeTi-AS model, did not lead to fracture of the neurocranium. However, the neurocranium in the CeTi-TS model did fracture based on maximum principal stress criteria.

ICP. When internal pressure was applied, there was negligible compression stress at the interface between the cranial implant and neurocranium.

DISCUSSION

Both the PEEK cranial implant and the CeTi implants were unable to withstand an external impact load of 18 kN. The maximum stress at the BSI of the PEEK implant and the application area of the CeTi cranial implants exceeded the strength of the materials and led to structural failure. High stress concentrations at the BSI of the PEEK cranial implant led to failure at the screw holes. Maximum stresses on the BSI of the PEEK implant were much higher than those on the CeTi implants. As PEEK exhibits non-osteoconductive properties, the only support between the implant and the bone is located at the fixation points; hence, stress accumulates at these points. Moreover, as the PEEK implant has a stiffness that is almost one-half of the stiffness of bone, the stresses are concentrated at the BSI of the bone as well. As these stresses exceed the ultimate strength of the bone, fracture of the neurocranium was observed at the screw holes. Nout et al[4] reported similar findings and suggested the use of biconcave washers to focus the force toward the screw shaft rather than toward the bone to reduce the stresses on the bone itself.

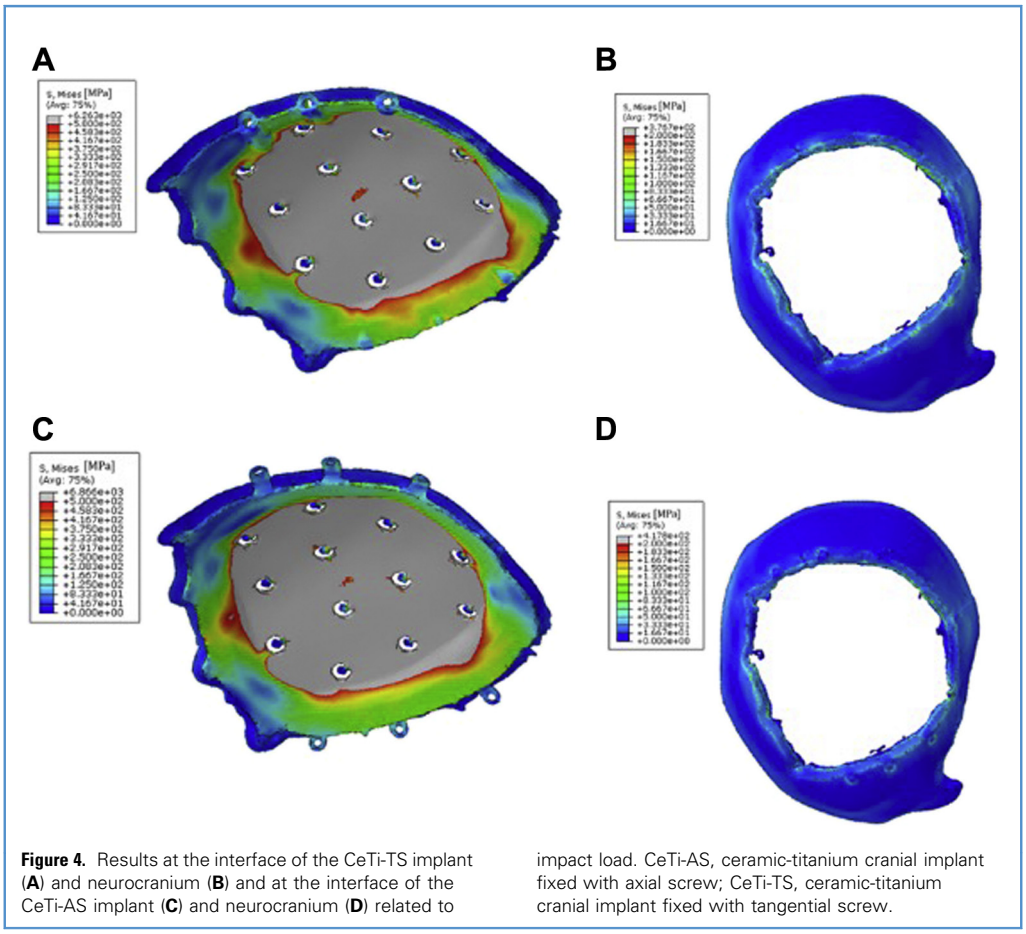

Figure 4. Results at the interface of the CeTi-TS implant (**A**) and neurocranium (**B**) and at the interface of the CeTi-AS implant (**C**) and neurocranium (**D**) related to impact load. CeTi-AS, ceramic-titanium cranial implant fixed with axial screw; CeTi-TS, ceramic-titanium cranial implant fixed with tangential screw.

In contrast to the high stresses at the interface of the PEEK cranial implant and neurocranium, reduced stresses at the BSI and BII-solid were observed when a CeTi implant was used. This result was observed in both the CeTi-TS and CeTi-AS models. The high stiffness of the Ti_6Al_4V alloy offers good load absorption; hence, stresses were concentrated at the center of the implant rather than at the perimeter.[4,16] The use of tangential screws in the CeTi models led to higher stresses at the BSI compared with the use of axial screws. The disparity in stresses can be attributed to the different contact areas between the tangential or axial screw hole and the neurocranium. The contact area of 1 tangential screw hole is approximately 20 mm^2 compared with 33 mm^2 for an axial screw hole. The use of tangential screws was reported to lead to higher strains due to the concentration of stress at the BSI.[4] Nevertheless, these authors claimed that tangential screws offer more rigid fixation compared with other methods, as the cranial implant is pulled into the defect.[4]

The maximum stress located at the BII-scaffold was lower than at the BII-solid, as the scaffold has a lower stiffness due to the combined properties of the Ti_6Al_4V lattice structure and HydroSet. The scaffold offers several advantages. First, stress shielding of the cranial bone is reduced as the stiffness of the scaffold is lower than solid Ti. Second, the presence of HydroSet enhances bone ingrowth. Previous studies have shown that the bioactivity and morphology of HydroSet, which are comparable to those of bone, contribute to a more rapid, stronger, and durable osseointegration.[17-20] The Ti lattice serves as a stable scaffold for the HydroSet, increasing the ability of the structure to maintain its integrity over time.[19] Furthermore, the high strength of the solid Ti_6Al_4V region at the center of the cranial implant is able to withstand an external impact load.

The von Mises and maximum principal stress criteria yield different outcomes. Based on the maximum principal stress, the neurocranium of the CeTi-TS implant fails, whereas the maximum von Mises stress does not exceed the strength of the bone. Hence, it is important that both criteria are investigated to provide a thorough view of the load-bearing capacity of the implants.

Indentation of the brain due to deflection of the cranial implant is a significant cause of brain injury.[21] When the implant material comes into contact with the meninges, an increase in brain pressure is observed. This increase in pressure, in combination with the deflection of the implant, further increases the stress imposed on the brain tissue.[9,22] Hence, an implant with a large deflection is more likely to indent the brain and cause injury.

Because of the low stiffness of the PEEK cranial implant, the maximum displacement at the application area is twice as high as that of the CeTi implants. Hence, the use of a PEEK implant increases the risk of brain injury when subjected to external impact loads, a finding that is supported by other studies.[4,9]

Another drawback of the PEEK implant is its thickness. The implant must be quite thick to have a strength and deflection comparable to that of native bone. This thickness may result in a larger increase in ICP compared with the (thinner) CeTi implant, which then leads to a severe reduction in blood perfusion to the brain.[15]

CONCLUSION

The results of this study show that the location and magnitude of stress and its displacement largely depend on the implant material and fixation method used. This work adds new findings to other state-of-the-art studies by comparing a PEEK implant with CeTi implants. The stress analyses show that, under an external impact load, CeTi implants are able to offer better neurocranial protection, as the maximum stresses are located at the center of the implant rather than at its perimeter, leading to a reduction in local stress concentrations at the interface. It is apparent that the use of tangential screws is a better choice than the use of axial screws, as the implant fixation is more stable. In addition, the HydroSet used in the scaffold structure allows enhanced bone ingrowth and results in a strong bond between the implant and neurocranium. Not only does the CeTi implant reduce the chance of neurocranial fracture, but it also offers better protection of the brain under an external impact load. Because of its high stiffness, the critical deflection of the CeTi implant is twice as low as that of the PEEK implant; hence, the risk of brain injury under an external load is decreased.

Additional research is recommended to further improve FEA outcomes, such as more accurately modeling the screws or the magnitudes of prestresses exerted by the screws, which would allow a better estimation of the magnitude of the stresses exerted at the BSI.

The results presented in this work provide information about the biomechanical behavior of cranial implants and can thus be used for design purposes to further improve the clinical outcomes of cranioplasties using these materials.

CRediT AUTHORSHIP CONTRIBUTION STATEMENT

Stijn E.F. Huys: Conceptualization, Methodology, Writing - review & editing, Supervision, Project administration. **Anke Van Gysel:** Methodology, Software, Validation, Formal analysis, Investigation, Resources, Data curation, Writing - original draft, Visualization. **Maurice Y. Mommaerts:** Conceptualization, Resources, Writing - review & editing, Supervision, Project administration. **Jos Vander Sloten:** Conceptualization, Methodology, Software, Resources, Writing - review & editing, Supervision, Project administration.

ACKNOWLEDGMENTS

We are grateful to Ing. Ruben Van de Sande and Benoit de Smet (CADskills BV) for providing the materials and data necessary for this project.

REFERENCES

1. Aydin S, Kucukyuruk B, Abuzayed B, Aydin S, Sanus GZ. Cranioplasty: review of materials and techniques. *J Neurosci Rural Pract*. 2011;2:162-167.
2. Khader BA, Towler MR. Materials and techniques used in cranioplasty fixation: a review. *Mater Sci Eng C Mater Biol Appl*. 2016;66:315-322.
3. Safi Y, Hohenberger S, Robbenmenke C, et al. Investigation of the failure behavior of a cranial implant-skull model under different load conditions using FEM. In: *SIMULIA Community Conference*. Spetzger; 2010:1-16.
4. Nout E, Mommaerts MY. Considerations in computer-aided design for inlay cranioplasty: technical note. *Oral Maxillofac Surg*. 2018;22:65-69.
5. Piazza M, Grady MS. Cranioplasty. *Neurosurg Clin N Am*. 2017;28:257-265.
6. Gordon DS, Blair GA. Titanium cranioplasty. *Br Med J*. 1974;2:478-481.
7. Wang YR, Su ZP, Yang SX, Guo BY, Zeng YJ. Biomechanical evaluation of cranial flap fixation techniques: comparative experimental study of suture, stainless steel wire, and rivetlike titanium clamp. *Ann Plast Surg*. 2007;58:388-391.
8. El Halabi F, Rodriguez JF, Rebolledo L, Hurtós E, Doblaré M. Mechanical characterization and numerical simulation of polyether-ether-ketone (PEEK) cranial implants. *J Mech Behav Biomed Mater*. 2011;4:1819-1832.
9. Tsouknidas A, Maropoulos S, Savvakis S, Michailidis N. FEM assisted evaluation of PMMA and Ti6Al4V as materials for cranioplasty resulting mechanical behaviour and the neurocranial protection. *Biomed Mater Eng*. 2011;21:139-147.
10. Mommaerts MY, Depauw PR, Nout E. Ceramic 3D-printed titanium cranioplasty. *Craniomaxillofac Trauma Reconstruct*. 2020;13:329-333.
11. Fahlstedt M, Baeck K, Halldin P, et al. Influence of impact velocity and angle in a detailed reconstruction of a bicycle accident. In: *International Research Council on Biomechanics of Injury*Proceedings of the International Research Council on the Biomechanics of Injury Conference (IRCOBI), Dublin. 40. 2012:787-799.
12. Diaz JM, Gonzalez-Estrada OA, Lopez CI. Biomechanical analysis of a cranial patient specific implant on the interface with the bone using the finite element method. In: *IFMBE Proceedings*. **60. Singapore: Springer; 2017:405-408.**
13. Bogu VP, Kumar YR, Khanara AK. Modelling and structural analysis of skull/cranial implant: beyond mid-line deformities. *Acta Bioeng Biomech*. 2017;19:125-131.
14. Clarkin OM, Boyd D, Madigan S, Towler MR. Comparison of an experimental bone cement with a commercial control, Hydroset. *J Mater Sci Mater Med*. 2009;20:1563-1570.

15. Boyd D, Towler MR, Wren A, Clarkin OM. Comparison of an experimental bone cement with surgical Simplex P, Spineplex and Cortoss. *J Mater Sci Mater Med*. 2008;19:1745-1752.

16. Savaser BO, Erogul OEO. Patient specific implant design and production for closure of skull defects. *EPSTEM*. 2017;1:22-29.

17. Kusakabe H, Sakamaki T, Nihei K, et al. Osseointegration of a hydroxyapatite-coated multilayered mesh stem. *Biomaterials*. 2004;25:2957-2969.

18. Ilea A, Vrabie OG, Băbțan AM, et al. Osseointegration of titanium scaffolds manufactured by selective laser melting in rabbit femur defect model. *J Mater Sci Mater Med*. 2019;30:26.

19. Ducic Y. Titanium mesh and hydroxyapatite cement cranioplasty: a report of 20 cases. *J Oral Maxillofac Surg*. 2002;60:272-276.

20. Jonkergouw J, van de Vijfeijken SE, Nout E, et al. Outcome in patient-specific PEEK cranioplasty: a two-center cohort study of 40 implants. *J Craniomaxillofac Surg*. 2016;44:1266-1272.

21. Safi Y, Hohenberger S, Robbenmenke C, et al. *Investigation of the failure behavior of a cranial implant-skull model under different load conditions using FEM*. Spettzger: SIMULIA Customer Conference; 2010:1-16.

22. Fujiwara S, Yanagida Y, Mizoi Y. Impact-induced intracranial pressure caused by an accelerated motion of the head or by skull deformation; an experimental study using physical models of the head and neck, and ones of the skull. *Forensic Sci Int*. 1989;43:159-169.

Conflict of interest statement: M. Y. Mommaerts is the innovation manager and co-owner of CADskills BV. S. E. F. Huys is the research and development officer at the same company. The remaining authors have no conflicts to report.

Received 14 November 2020; accepted 21 January 2021

Citation: World Neurosurg. (2021) 148:■-■.
https://doi.org/10.1016/j.wneu.2021.01.102

Journal homepage: ***www.journals.elsevier.com/world-neurosurgery***

Available online: ***www.sciencedirect.com***

1878-8750/$ - see front matter *© 2021 Elsevier Inc. All rights reserved.*